3-2004

Folding Kinetics and Structure of OEP16

Dirk Linke

Joachim Frank

Matthew S. Pope

Jurgen Soll

Iryna Ilkavets

See next page for additional authors

Citation/Publisher Attribution

Linke, D., Frank, J., Pope, M. S., Soll, J., Ilkavets,I., Fromme, P., Burstein, E. A., & Reshetnyak, Y. (2004). Folding Kinetics and Structure of OEP16. *Biophys. J.*, *86*(3), 1479-1487. doi: 10.1016/S0006-3495(04)74216-2

Available at: http://dx.doi.org/10.1016/S0006-3495(04)74216-2

Folding Kinetics and Structure of OEP16

Dirk Linke,* Joachim Frank,* Matthew S. Pope,† Jürgen Soll,‡ Iryna Ilkavets,‡ Petra Fromme,§ Edward A. Burstein,¶ Yana K. Reshetnyak,|| and Victor I. Emelyanenko¶

*Max Volmer Laboratorium, Institut für Chemie der Technischen Universität Berlin, 10623 Berlin, Germany; †Applied Photophysics, Leatherhead, Surrey, KT22 7PB, United Kingdom; ‡Botanisches Institut, Ludwig-Maximilians-Universität München, 80638 Munich, Germany; §Department of Chemistry and Biochemistry, Arizona State University, Tempe, Arizona 85287-1604 USA; ¶Institute of Theoretical and Experimental Biophysics, Russian Academy of Sciences, 142290 Pushchino, Moscow Region, Russia; and ||Department of Molecular Biology and Immunology, University of North Texas Health Science Center, Fort Worth, Texas 76107 USA

ABSTRACT The chloroplast outer membrane contains different, specialized pores that are involved in highly specific traffic processes from the cytosol into the chloroplast and vice versa. One representative member of these channels is the outer envelope protein 16 (OEP16), a cation-selective high conductance channel with high selectivity for amino acids. Here we study the mechanism and kinetics of the folding of this membrane protein by fluorescence and circular dichroism spectroscopy, using deletion mutants of the two single tryptophanes Trp-77→Phe-77 and Trp-100→Phe-100. In addition, the wild-type spectra were deconvoluted, depicting the individual contributions from each of the two tryptophan residues. The results show that both tryptophan residues are located in a completely different environment. The Trp-77 is deeply buried in the hydrophobic part of the protein, whereas the Trp-100 is partially solvent exposed. These results were further confirmed by studies of fluorescence quenching with I^-. The kinetics of the protein folding are studied by stopped flow fluorescence and circular dichroism measurements. The folding process depends highly on the detergent concentration and can be divided into an ultrafast phase ($k > 1000\ s^{-1}$), a fast phase (200–800 s^{-1}), and a slow phase (25–70 s^{-1}). The slow phase is absent in the W100F mutant. Secondary structure analysis and comparision with closely related proteins led to a new model of the structure of OEP16, suggesting that the protein is, in contrast to most other outer membrane proteins studied so far, purely α-helical, consisting of four transmembrane helices. Trp-77 is located in helix II, whereas the Trp-100 is located in the loop between helices II and III, close to the interface to helix III. We suggest that the first, very fast process corresponds to the formation of the helices, whereas the insertion of the helices into the detergent micelle and the correct folding of the II-III loop may be the later, rate-limiting steps of the folding process.

INTRODUCTION

The chloroplast outer envelope is a membrane system with a high lipid/protein ratio (Joyard et al., 1991) containing enzymes for lipid biosynthesis (Block et al., 1983; Froehlich et al., 2001), the machinery for protein import into the organelle (Cline and Henry, 1996; Heins et al., 1998), and transport proteins for substrates and products of all kinds of biosynthetic pathways. In contrast to the very specific and sometimes energy-consuming transport processes across the inner envelope (Flügge, 1998), it seems that the solute exchange across the outer membrane is driven mainly by diffusion. In older textbooks, large pore proteins of the porin type were postulated, which made the membrane leaky for all kinds of substances having a molecular mass lower than 10 kDa. Today, different and highly specific pores have been identified (Pohlmeyer et al., 1997, 1998; Bölter et al., 1999). The existence of these pores suggests complex solute selectivity and regulation processes (Flügge, 2000; Soll et al., 2000).

OEP16, the 16-kDa outer envelope protein from pea chloroplasts, is a cation-selective high-conductance channel with a remarkable selectivity for amino acids and amines (Pohlmeyer et al., 1997). It has sequence homologies to LivH, an amino acid transporter of *Escherichia coli*, as well as to Tim22, Tim23, and Tim17, subunits of the preprotein translocase of the mitochondrial inner membrane. These proteins, together with OEP16, are thought to form a closely related family of preprotein and amino acid transporters (Rassow et al., 1999). The Tim proteins all consist of four transmembrane α-helices, and their similarity to OEP16 extends over almost the whole sequence but is strongest in a 52 amino acid region around helices II and III, where it reaches 50% (Rassow et al., 1999).

Through the use of spectroscopic methods, OEP16 in the presence of detergents has been shown to fold into the same native-like structure as in liposomes (Linke et al., 2000), where its function can be and was assayed (Pohlmeyer et al., 1997). Cross-link experiments suggest OEP16 to be a homodimer, and on this basis, a structural model with a mixed β-sheet/α-helix transmembrane domain was proposed based on circular dichroism (CD) spectroscopy data and hydropathy plots (Pohlmeyer et al., 1997). After mutagenesis experiments identified the pore-forming part of the protein, a new model of an at least tetrameric β-barrel was discussed (Steinkamp et al., 2000) based on the fact that a transmembrane helix could not be identified in that region by standard secondary structure prediction and hydropathy plots.

Submitted July 15, 2003, and accepted for publication November 21, 2003.

Address reprint requests to Petra Fromme, Fax: +1-480-965-2747; E-mail: petra.fromme@asu.edu; or Dirk Linke, E-mail: dirk.linke@tuebingen.mpg.de.

Dirk Linke's present address is Max Planck Institute for Developmental Biology, Dept. I, Protein Evolution, Spemannstr. 35 D-72076 Tübingen, Germany.

0006-3495/04/03/1479/09 $2.00

OEP16 contains two tryptophan residues that primarily contribute to the fluorescence spectrum at 280-nm excitation wavelength. Here we describe the contribution of the single tryptophan residues to the complete wild-type (WT) spectrum by using two mutants, Trp-77→Phe-77 (W77F) and Trp-100→Phe-100 (W100F). By deconvoluting the fluorescence spectra of the wild-type OEP16 and analyzing the spectra of the mutants, we show that the tryptophan residues belong to distinct structural classes as described by Burstein et al. (2001; Reshetnyak and Burstein, 2001; Reshetnyak et al., 2001). Finally, stopped-flow experiments with wild type and mutants gave insights into the folding kinetics of the protein. A new structural model of a purely α-helical OEP16 is proposed from sequence similarities and new secondary structure predictions.

MATERIALS AND METHODS

Single tryptophan mutants

To obtain single tryptophan mutants, polymerase chain reaction (PCR)-based site directed mutagenesis was used. In the first step, two separate PCR reactions were performed for each mutant. The OEP16 cDNA inserted in the PET21b expression vector was used as a template. The primers were

1. OEP16W77/FN 5′-GCC GGC TAT AGC TCC **GAA** GTA TGC ACC TTC-3′ and a T7 promoter primer;
2. OEP16W77/FC 5′-GAA GGT GCA TAC **TTC** GGA GCT ATA GCC GGC-3′ and a T7 terminator primer;
3. OEP16W100/FN 5′-CAT GGC ATT CTT **GAA** CTC CCT GGT GCC ACG-3′ and a T7 promotor primer;
4. OEP16W100/FC 5′-CGT GGC ACC AGG GAC **TTC** AAG AAT GCC ATG-3′ and a T7 terminator primer.

Changes in the nucleotide sequence compared to the wild type are in bold letters. The fragments for the W77F and W100F mutants were then annealed together in a second PCR step to amplify the complete mutated gene using T7 promoter and terminator primers. The resulting PCR products were digested with *Nde*I and *Xho*I restriction enzymes and ligated into the corresponding sites of the pET21b expression vector. They were named W77F-pET21b and W100F-pET21b, respectively. The correct mutations were confirmed by sequencing.

Overexpression and protein purification

Overexpression of wild-type and recombinant proteins was performed as described (Pohlmeyer et al., 1997). Protein was isolated from *E. coli* cells as inclusion bodies and was purified by ion exchange chromatography in an unfolded state in a buffer containing 6 M urea (Linke et al., 2000). Protein concentrations were determined by the method of Bradford (Bradford, 1976).

Protein reconstitution

To obtain correctly folded OEP16, the protein-containing urea buffer was diluted 1:10 with a buffer containing 20 mM HEPES/KOH pH 7.6, 1 mM EDTA, and 0.03% octaethyleneglycol-monododecylether ($C_{12}E_8$) (Linke et al., 2000). The final protein concentration was 0.1–0.3 mg/ml.

Fluorescence measurements

Fluorescence measurements were performed in an ISA Fluoromax-2 fluorescence spectrometer (ISA-SPEX, Edison, NJ) in halfmicro quartz cells (sample volume 1 ml, optical path 1 cm). The spectral widths of both the excitation and the emission bands were 2 nm. Excitation was performed at 295 nm wavelength to exclude presence of tyrosine fluorescence in the spectra. Emission spectra were recorded from 305 to 500 nm in 0.5-nm steps. Five spectra measured independently were averaged. To obtain quenched spectra, KI or CsCl was added to final concentrations ranging from 100 to 500 mM. An emission spectrum of a neutral aqueous solution of L-tryptophan was used as a standard for the correction of protein spectra relating to the instrument's spectral sensitivity (Burstein and Emelyanenko, 1996). The intensities of the corrected spectra are proportional to the number of photons emitted per unit wavelength interval.

Deconvolution of fluorescence spectra

The shape of an ''elementary'' component of protein fluorescence spectra on the frequency (wavenumber) scale was approximated by the uniparametric log-normal function (Burstein and Emelyanenko, 1996). The deconvolution into components was performed on sets of spectra measured at various quencher concentrations (KI and/or CsCl) using the SIMS and PHREQ algorithm (Abornev and Burstein, 1992; Burstein et al., 2001). The spectra were independently fitted by one, two, or three components. The criterion of attaining the best solution (i.e., a solution with a sufficient number of components) was the minimal root-mean-square differences (residuals) between theoretical and experimental spectra. For each i-th component, the program output data contained the values of the maximal spectral position $\lambda_{max}(i)$, the percent contribution of the component into the area under total spectrum $S(i)$, the Stern-Volmer quenching constant $K_{SV}(i)$, and its ratio to the K_{SV} value for quenching free aqueous tryptophan emission with the same quencher, $K_{rel}(i)$. The maximal position of the total protein fluorescence spectrum was taken from the one-component log-normal description of the spectrum shape. The Stern-Volmer constants, $K_{SV}(i)$, were calculated as slopes of the linear plots in coordinates $(A_0/A_c - 1)$ versus quencher chemical activity (Burstein et al., 2001), where A_0 and A_c are the areas under the emission component spectra measured in the absence (A_0) and presence of a quencher in the concentration c (A_c). To calculate K_{rel} values, the K_{SV} values for dynamic quenching of free aqueous tryptophan emission with iodide and cesium were taken to be 12.8 and 2.8 M^{-1}, respectively (Bukolova-Orlova et al., 1974; Bushueva et al., 1974).

Stopped-flow measurements with fluorescence detection

The time-dependent intensity changes of the tryptophan fluorescence of OEP16 during the folding process was measured between 1 and 100 ms by using a SX-18MV stopped-flow apparatus (Applied Photophysics, Leatherhead, UK) in the ratio mixing mode. The excitation of the tryptophan fluorescence was achieved by a 150-W high pressure xenon arc lamp at a wavelength of 280 ± 20 nm. The detection of the fluorescence was performed at a wavelength of 334 nm through an interference filter with a spectral bandwidth of 10 nm (L.O.T. Oriel GmbH, Darmstadt, Germany). The fluorescence changes were recorded after fast 1:10 mixing of an OEP16 solution containing 6 M urea, 20 mM HEPES at pH 7.6, and 1 mM EDTA with a detergent-rich 20 mM HEPES buffer (1 mM EDTA) at pH 7.6. The detergent and protein concentrations after mixing were between 0.003 and 0.03% w/v for $C_{12}E_8$ and 0.07 mg/ml for OEP16, respectively. The resulting stopped-flow signals were fitted via nonlinear regression to double-exponential equations in the time range between 3 and 100 ms.

Stopped-flow experiments with CD detection

Time-resolved CD measurements relating to the refolding of OEP16 were performed with a π^*-180 CD stopped-flow spectrometer manufactured by Applied Photophysics at a wavelength of 228 nm and a pathlength of 2 mm.

After rapid mixing of the OEP16 solution in a ratio of 1:10 with a detergent-rich buffer of 20 mM HEPES at pH 7.6 containing 0.01–0.03% $C_{12}E_8$ and 1 mM EDTA, the transient change in ellipticity was recorded between 2 and 200 ms.

Hydrophobic cluster analysis

Hydrophobic cluster analysis (Callebaut et al., 1997) was performed with the web-based tool at http://smi.snv.jussieu.fr/hca/hca-seq.html to visualize the hydrophobicity of the environment of the two tryptophan residues in OEP16 wild type.

RESULTS

Decomposition of fluorescence spectra

The protein fluorescence of OEP16 is sensitive to the environment of the two tryptophan residues of this membrane protein. Upon refolding after dilution of OEP16 in detergent-rich buffer solutions the protein fluorescence increases with time and becomes shifted to shorter wavelengths (Linke et al., 2000). To study the contribution of the two tryptophan residues to this effect, we measured fluorescence spectra of the refolded wild-type protein and two single-tryptophan mutants. Fig. 1 *a* shows the fluorescence spectra of refolded OEP16 dissolved in 0.03% $C_{12}E_8$ with 0.6 M urea (20 mM HEPES at pH 7.6 and 1 mM EDTA) and of the single tryptophan mutants OEP16 W77F and W100F. Although the wild-type spectrum has its fluorescence maximum at 336-nm wavelength, the spectra of W77F and W100F have peaks at 340 and 333 nm, respectively. When summing up the two mutant spectra at equal protein concentrations, the calculated spectrum is almost identical in shape to the wild-type spectrum, even though its intensity is stronger. On the other hand, mathematical decomposition of the fluorescence spectrum of wild-type OEP16 into log-normal components (see Materials and Methods) yielded again two components

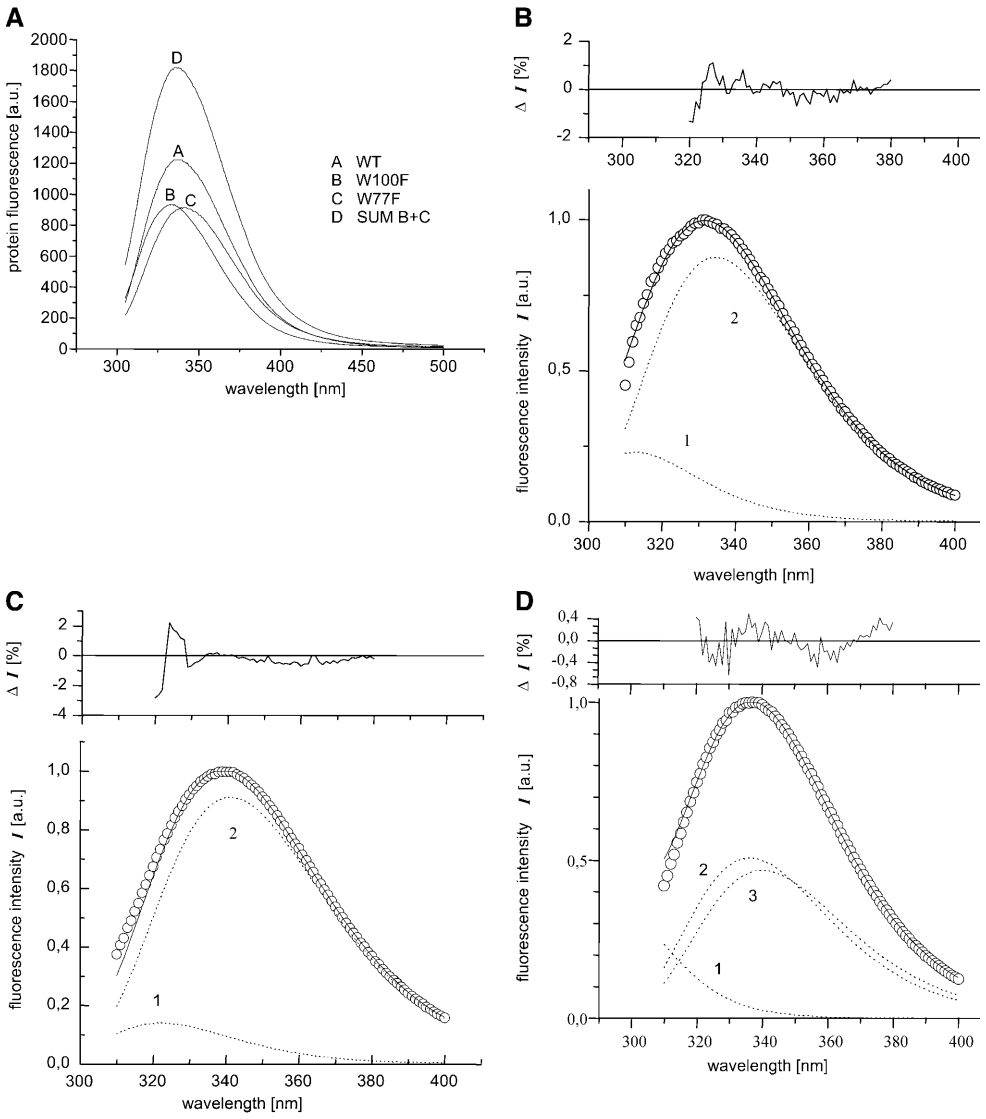

FIGURE 1 Fluorescence spectra of OEP16, its single-tryptophan mutants, and results of their decomposition into log-normal spectral components. (*A*) Fluorescence spectra of OEP16 WT (*A*), W100F (*B*), W77F (*C*), and the sum of B + C (*D*). (*B–D*) Decomposition of fluorescence spectra of mutant W100F (*B*), mutant W77F (*C*), and wild-type OEP16 (*D*) into the log-normal components (*dotted curves 1*, *2*, and *3*) in the absence of any quencher. Upper spectra: experimental points (○); the sum of log-normal components (*solid curves*). In the top panel are presented the percent residuals between sum of component spectra and experimental emission intensities in the wavelength range used for the decomposition (320–380 nm). See also Table 1 for results.

belonging to tryptophan residues 77 and 100 and an additional very short-wavelength component that cannot be attributed to a tryptophan fluorophore (Fig. 1 *d*); the component most likely belongs to the stray excitation light. Decomposition of the spectra of W100F (Trp-77) and W77F (Trp-100) each yielded only one tryptophan component (Table 1; Fig. 1, *b* and *c*), again with an additional non-tryptophan component that is most likely a buffer and detergent impurity and/or the stray light. Although the shape of the spectrum of stray light and/or emission of impurities must not be described with the log-normal function used for the tryptophan emission spectra, a special test showed that a variation of the spectral shape of the shortest-wavelength components resulted in minimal (± 1 nm) changes in the maximal position of longer-wavelength components belonging to tryptophan residues. Thus, the two tryptophan residues contribute independently to the wild-type spectrum, and their contributions can be observed in the single-tryptophan mutants. This is especially helpful in stopped-flow experiments with fluorescence detection, where only a fixed wavelength can be monitored.

According to references (Burstein et al., 2001; Reshetnyak and Burstein, 2001; Reshetnyak et al., 2001), tryptophan fluorophores in proteins can be divided into five discrete classes with respect to their emission maxima and features of the indole fluorophore microenvironment. Using this classification, Trp-100 (λ_{max} ~340 nm) belongs to class II and is partially exposed to bound water, and Trp-77 is a class I fluorophore largely buried in the nonpolar environment of the protein. Class I fluorophores may only occasionally interact with bound water but are not exposed to the solvent. The different accessibilities to the solvent can also be shown by quenching experiments. Panels *a* and *b* of Fig. 2 show the Stern-Volmer plots for the quenching of the log-normal components of the wild-type OEP16 by iodide ions. The fluorescence of Trp-100 is more strongly quenched compared to Trp-77. Trp-100 is therefore more exposed to the solvent than Trp-77. This fact is quantified by the values of the relative Stern-Volmer constants K_{SV} (K_{rel}) for the iodide quenching of the emission of Trp-77 ($K_{rel} = 5.6 \pm 1.7\%$) and Trp-100 ($K_{rel} = 13.1 \pm 2.2\%$) in the corresponding OEP16 mutants (Table 1; Fig. 2). On the other hand, the K_{rel} value for quenching Trp-100 emission by positively charged Cs^+

TABLE 1 Maxima of experimental and calculated fluorescence spectra

	Experimental emission maximum (nm)	Log-normal components maximum (nm)		K_{rel} (%)
Wild-type OEP16	336	336.2	340.0	–
W100F (Trp-77)	333	335.4	–	5.6 (KI)
W77F (Trp-100)	339	–	341.1	13.1 (KI)
				21.1 (CsCl)

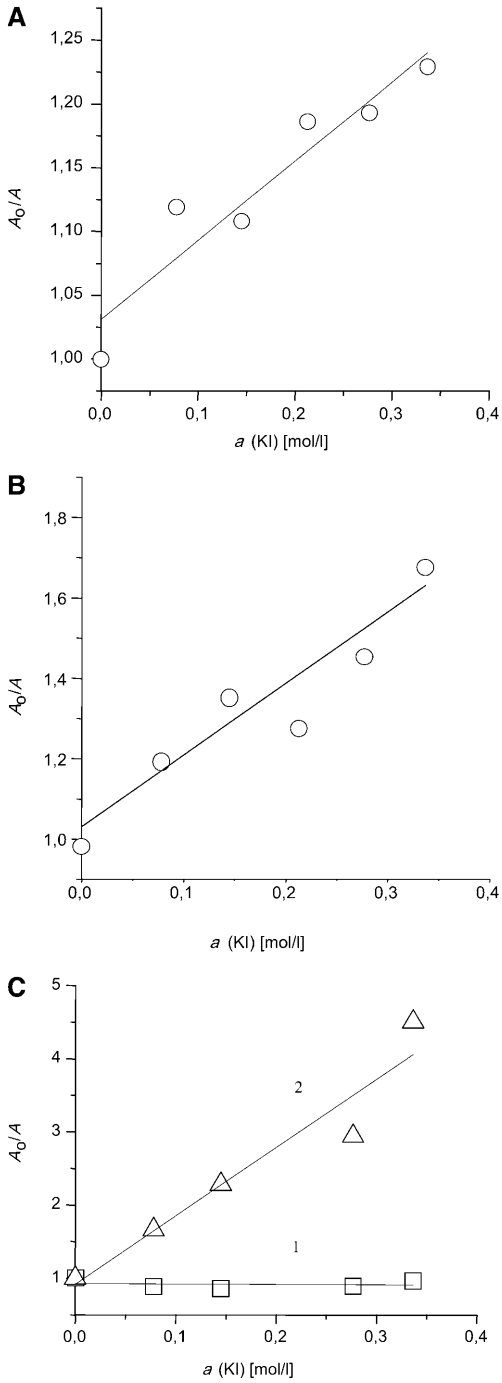

FIGURE 2 Stern-Volmer plots for KI quenching of main log-normal components belonging to tryptophan residues in fluorescence spectra of mutants W100F (*A*) and W77F (*B*) and wild-type OEP16 (*C*). The plots 1 and 2 in *C* correspond to the components plotted as spectra 2 ($\lambda_{max} = 336.2$ nm) and 3 ($\lambda_{max} = 340.0$ nm) of Fig. 1 *D*, respectively. Abscissas: chemical activities of KI. Ordinates: the ratio of full areas (integrals) under component spectra measured without KI (A_0) and at a given quencher activity *a* (*A*). Points (○) are calculated A_0/A versus *a*; the straight lines are the linear regressions of the points. See also Table 1 for results.

is essentially higher (21.1 ± 7.0%) than it is in the case of quenching by negatively charged iodide. That means that the protein surface nearby Trp-100 bears a somewhat negative electrostatic charge, most likely represented by Asp-99.

Stopped-flow measurements (fluorescence/CD)

In the unfolded state the maximal emission of the tryptophan fluorescence of wild-type OEP16 is 355 nm. Refolded wild-type OEP16 exhibits a stronger tryptophan fluorescence with a maximum at 336 nm in the presence of 0.03% w/v $C_{12}E_8$. Complete folding is achieved below urea concentrations of ~1.5 M, whereas total exposure of the tryptophan residues to the hydrophilic solvent, in the denatured state, is complete at urea concentrations higher than 5 M (Linke, 2002). If the reaction is not faster than ~1 ms, the time resolution of a stopped-flow apparatus should be sufficient to follow the time course of the folding reaction via the fluorescence increase at 335 nm. In fact, refolding of OEP16 is a fast process that is finished in 100 ms under conditions known to give high yields of renaturation in the presence of 0.03% w/v $C_{12}E_8$ (Linke et al., 2000). Refolding of wild-type OEP16 from the denatured state at 6 M urea by dilution of 1:10 with $C_{12}E_8$/buffer solutions generally produces double-phasic stopped-flow signals with an increase of fluorescence intensity at 334 ± 5 nm. The kinetics of the different folding processes of wild-type OEP16 are pseudofirst-order with respect to the $C_{12}E_8$ concentration. Below the critical micellation concentration (CMC) of $C_{12}E_8$ (0.11 mM or 0.006%, respectively) a folding reaction could not be observed. Only at very low detergent concentrations above the CMC can three processes be fit to the then triple-exponential curve. The fastest process is only visible at $C_{12}E_8$ concentrations of 0.01% w/v and less and is poorly resolved (data not shown). At higher detergent concentrations this process becomes faster than the time resolution (1.3 ms) of the stopped-flow apparatus. To reduce the influence of the fastest signal we started the nonlinear regression fitting procedure at 3 ms to determine the rate constants of the two slower processes.

The observed rate constants ($k_{obs} = 1/\tau$) of the two well-resolved processes increase linearly with $C_{12}E_8$ concentrations between 0.01 and 0.03% w/v, reaching 830 ± 200 s^{-1} and 60 ± 17 s^{-1} at 0.03% w/v $C_{12}E_8$ (Figs. 3 *a*, WT trace, and 4, *a* and *b*; see also Table 2).

At low $C_{12}E_8$ concentrations the two slower processes possess similar amplitudes, whereas at higher $C_{12}E_8$ concentrations the faster process dominates (Fig. 4 *c*). Double exponential fits of the stopped-flow signals in the time range between 3 and 100 ms suggest that the slowest process reaches a maximal amplitude close to the CMC value of $C_{12}E_8$, and declines with higher $C_{12}E_8$ concentrations, where the amplitude of the faster process increases with increasing $C_{12}E_8$ concentration. The time constants of both processes are independent of the protein concentration, tested for OEP16 concentrations ranging from 0.2 to 2 mg/ml (Fig. 4 *d*).

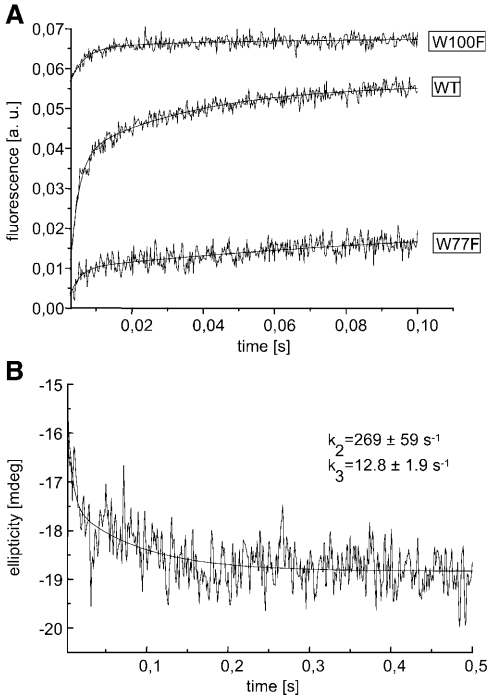

FIGURE 3 (*A*) Stopped-flow fluorescence traces recorded at 334 nm with a detergent concentration of 0.01% $C_{12}E_8$. Protein concentration is 0.07 mg/ml OEP16. Two processes with first-order kinetics can be fitted (one for W100F). For results, see Table 2. (*B*) Stopped-flow CD trace recorded at 225-nm wavelength with a detergent concentration of 0.01% $C_{12}E_8$ at 0.08 mg/ml OEP16. For time constants for the two processes, see Table 2.

We confirmed the stopped-flow experiments using fluorescence detection by applying time-resolved circular dichroism measurements under comparable conditions (Fig. 3 *b*). Time-resolved CD measurements monitored the refolding of wild-type OEP16, which was associated with an increase of the CD signal at 228-nm wavelength on the same timescale as observed with fluorescence detection (Table 2). The increase in the CD signal corresponded to a time-dependent decrease in ellipticity at a wavelength typical for α-helical signals. Again, triple exponential signals are observed at very low detergent concentrations. The fastest process that is beyond the time resolution of the CD stopped-flow apparatus can be seen only at 0.01% w/v

TABLE 2 Time constants of the stopped-flow experiments measured at 0.01% $C_{12}E_8$, 0.7 mg/ml OEP16

	k_2 (s^{-1})	k_3 (s^{-1})
	With fluorescence detection	
WT	427 ± 30	29.0 ± 2.2
W100F (Trp-77)	255 ± 57	–
W77F (Trp-100)	377 ± 135	8.0 ± 5.8
	With CD detection	
WT	269 ± 59	12.8 ± 1.9

All fits started at 3 ms; two first-order processes best describe the fit curve (one process for W100F). Note that a third, very fast process, k_1, is present that cannot be properly evaluated with the given methods (see text).

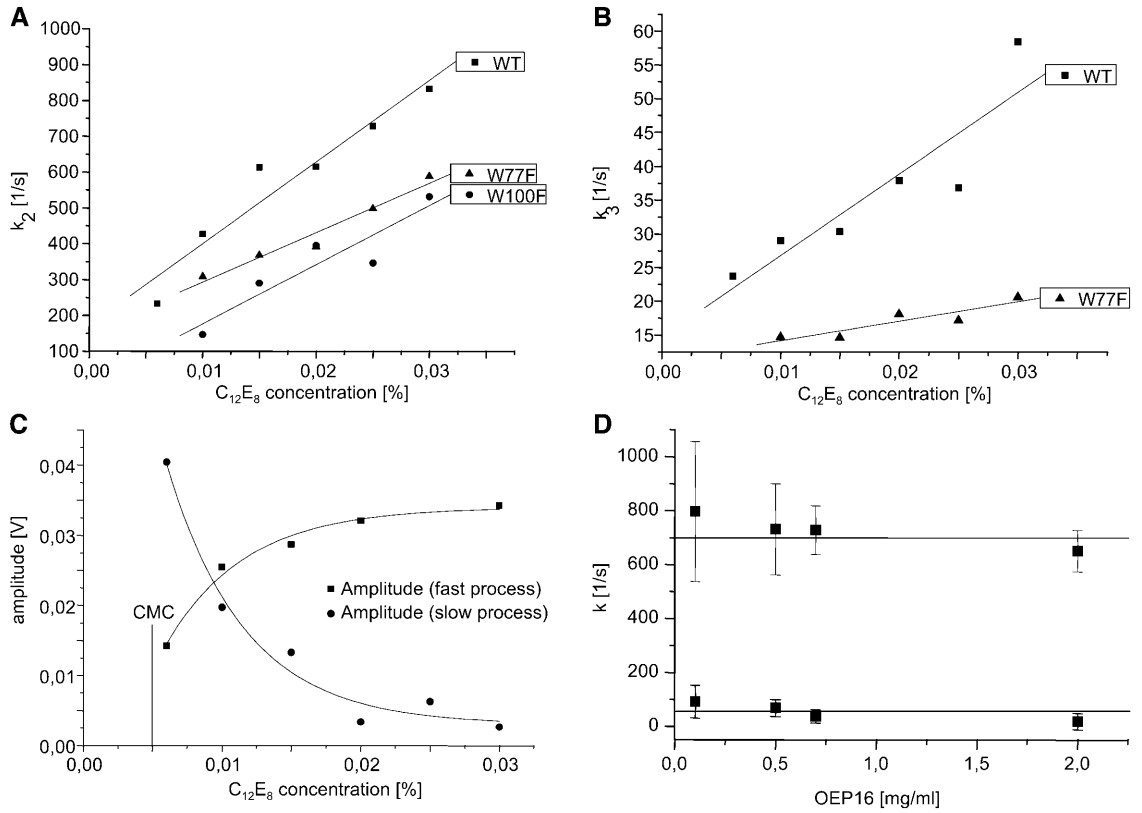

FIGURE 4 Time constants of the faster (*A*) and slower (*B*) folding processes of OEP16 as a function of the detergent concentration as observed in fluorescence stopped-flow measurements. *C* shows the amplitudes of the processes in V photomultiplier voltage. The independence of the rate constants from the protein concentration is visualized in *D*.

$C_{12}E_8$. The k_{obs} of the second process (k_2) measured with CD detection at 0.03% w/v $C_{12}E_8$ was determined to be 660 ± 170 s^{-1}. The second process is linearly dependent on the $C_{12}E_8$ concentration between 0.01 and 0.03% w/v. The third signal is slow, with ~50% of the total amplitude at low $C_{12}E_8$ concentrations (0.01% w/v), but the amplitude decreases at higher $C_{12}E_8$ concentrations, where the faster process dominates, just as in the fluorescence measurements.

In contrast to wild-type OEP16, the single tryptophan residue containing recombinant protein W100F misses the slowest relaxation phase of the folding process. This shows that the folding of OEP16 can occur in two steps and Trp-100 can be used as an indicator for the rate limiting second folding event. The stopped-flow traces for the refolding of OEP16 W100F are best described with single exponentials in the time range between 3 and 100 ms. Biexponential fits of the stopped-flow traces do not improve the normalized variance compared with monoexponential fits. Again, a very fast process can be seen for low detergent concentrations, and, as for the wild-type protein, it cannot be properly resolved. The second process is as fast as it is for wild-type OEP16, reaching a value of $k_2 = 530\ s^{-1}$ at 0.03% $C_{12}E_8$ and 25°C (Fig. 4 *a*). This process is pseudofirst-order with respect to the detergent concentration as observed for wild-type OEP16.

OEP16 W77F again shows double/triple phasic stopped-flow traces for the folding reaction as observed for wild-type OEP16. In the time range between 3 and 100 ms the stopped-flow signals are best described with double exponential fit functions that yield significantly better values for the normalized variance compared with single exponential fits. Again, the fastest process is beyond the time resolution of the stopped-flow apparatus. The observed rate constants of the second and third processes are comparable to the corresponding rate constants of the folding reactions for wild-type OEP16 with $k_2 = 588\ s^{-1}$ (Fig. 4 *a*) and $k_3 = 20.6\ s^{-1}$ (Fig. 4 *b*) at 0.03% $C_{12}E_8$ and 25°C. Both processes are pseudofirst-order with respect to the detergent concentration, as observed for wild-type OEP16. The amplitude of the second process increases with detergent concentration, whereas the amplitude of the slowest process declines in the concentration range studied, as in the wild type.

DISCUSSION

OEP16 contains only two tryptophan residues that are located in different structural environments (Trp-77 and Trp-100). Decomposition of the protein fluorescence spectrum of OEP16 yielded two distinct components that can be related to Trp-77 and Trp-100. Due to a low solvent

accessibility the fluorescence of Trp-77 is blue shifted compared to residue Trp-100. According to Burstein and co-workers, tryptophan fluorophores in proteins can be divided into five discrete classes with respect to their emission maximum (Burstein, 1983; Burstein et al., 2001; Reshetnyak and Burstein, 2001; Reshetnyak et al., 2001). Trp-77 belongs to class I (buried tryptophan fluorophores scarcely accessible except to bound water), whereas Trp-100 is a class II fluorophore partially solvent exposed. Therefore, Trp-77 fluorescence is not as strongly quenched by I^- ions as observed for Trp-100. The very short wavelength component visible after decomposition of the emission spectra of wild-type OEP16 and the single tryptophan mutants is not assigned to a tryptophan fluorophore. It is probably due to a buffer contamination and/or the stray excitation light.

Fig. 5 *a* shows a hydrophobic cluster analysis plot of OEP16. Hydrophobic cluster analysis can be used to visualize the environment of amino acid residues within transmembrane α-helices and β-sheets (Callebaut et al., 1997). The transmembrane α-helices, as predicted by hydropathy plots, mutagenesis experiments (Steinkamp et al., 2000), and other bioinformatics methods that involved analysis of OEP16 homologs from other plants (Linke, 2002), are highlighted in gray and are numbered I–IV from the N- to C-terminus, in accordance with helix nomenclature in the proteins of the Tim family (Rassow et al., 1999). Hydrophobic regions are in hexagonal boxes. Fig. 5 *b* shows the resulting topology model.

Helix I is responsible for substrate specifity and, together with helix II, for pore formation. It is amphiphilic due to its partial exposure to the water-filled pore, containing two charged residues in the middle of the membrane and has therefore been predicted as a β-sheet structure (Pohlmeyer et al., 1997; Steinkamp et al., 2000). But the high similarity to Tim22 and other Tim proteins that are purely α-helical and to LivH, an amino acid transporter of the *E. coli* inner membrane make a completely helical structure much more probable than a thermodynamically unfavorable mixed helix/sheet structure or a tetrameric β-barrel.

Trp-77 is part of a transmembrane α-helix (helix II) with several hydrophobic amino acids in its vicinity (Steinkamp et al., 2000; Linke, 2002). In mutagenesis experiments, it could be exchanged with helix IV without impairing pore activity (Steinkamp et al., 2000). This shows that helix II is structurally important but is not directly involved in the formation of the pore. Trp-100 is part of a loop region located adjacent to transmembrane helix III. It is not located within the pore-forming part of the protein, as has been shown with deletion mutants (Steinkamp et al., 2000).

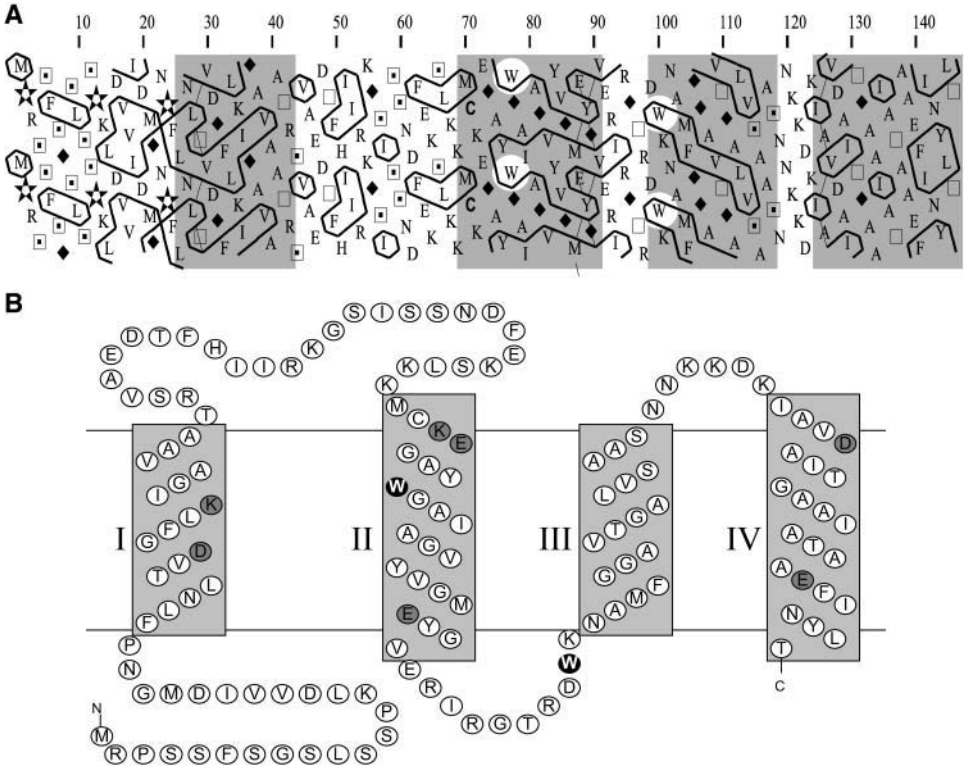

FIGURE 5 (*A*) Hydrophobic cluster analysis. The α-helices of OEP16 are highlighted in gray. The two tryptophan residues in helices II and III are marked (○). W77 is embedded in a more hydrophobic environment than W100. (*B*) Topology model for OEP16. The tryptophan residues are highlighted, as are charged residues within the predicted transmembrane helices. Note that only helix I contains charged residues in a central position and that the exchangeable (Steinkamp et al., 2000) helices II and IV have similar patterns of charged residues at their ends.

It can be seen that Trp-77 lies embedded between hydrophobic residues in the middle of a helix, whereas Trp-100 is located at the start of the next transmembrane segment. This indicates that the environment of Trp-77 is more hydrophobic than that of Trp-100. The results of the secondary structure prediction methods are in close agreement with the observed stronger blue shift of the tryptophan fluorescence of Trp-77 and the quenching experiments.

The folding of α-helical and β-barrel membrane proteins within lipid bilayers can be described by the partial formation of secondary structure motifs followed by the insertion of the membrane protein into the lipid bilayer (Booth and Curran, 1999; Buchanan, 1999; Schulz, 2000). The insertion process is slow, with a half-time in the range of minutes (Kleinschmidt and Tamm, 1996). Detergent micelles are known to include hydrophobic compounds and solubilize membrane proteins by shielding hydrophobic parts of the protein against the polar solvent (Timmins et al., 1994). The formation and breakdown of micelles is a dynamic equilibrium state with lifetimes for the micelles in the order of 1 ms (Kuni et al., 2001a,b). The incorporation of hydrophobic compounds in micelles can be as fast as the lifetime of the micelle. We assume that detergent-assisted refolding of OEP16 cannot be faster than the incorporation of this small membrane protein into the $C_{12}E_8$ micelle, which has a molecular mass of ~60,000 Da (Danino et al., 1997). The refolding of OEP16 probably starts immediately after embedding the hydrophobic parts of the membrane protein into detergent, leading to the observation of very fast refolding kinetics in the millisecond range.

The folding process of OEP16 is monitored by measuring the blue shift and the increase of the tryptophan fluorescence upon refolding. Single-tryptophan mutants of OEP16 are excellent objects for studying the folding reaction and allow us to study this process in greater detail. Additional time-resolved CD measurements confirmed that the observed fluorescence changes correspond to the formation of secondary structure elements during the folding process (Fig. 3 *b*).

Three steps should lead to completely folded OEP16 protein. First, helices start to form. In a second step, these helices are inserted into the hydrophobic environment of the detergent micelle. Finally, some rearrangement of loops and helices may take part. These rearrangements can also include oligomerization. The proof of this possibility will be subject for further investigations.

The observed stopped-flow traces with fluorescence (Fig. 3 *a*) or CD detection (Fig. 3 *b*) consist of three steps in the case of wild-type OEP16. OEP16 W100F is lacking the slowest relaxation process, whereas OEP16 W77F shows all three processes. Unfortunately, the fastest process is faster than the time resolution of the stopped-flow experiment and thus cannot be resolved properly.

We assume that the rate constants for the formation (step 1) and insertion (step 2) of helices II and III are comparable. A very fast and a fast process with comparable rate constants are visible in both mutants. They are so similar that they cannot be distinguished from each other in the wild-type fluorescence traces with contributions from both Trp residues.

The fastest process does not reflect the increase in hydrophobicity upon mixing OEP16 with $C_{12}E_8$ micelles as it does in the case of refolding of bacteriorhodopsin in 1,2-dimyristoyl-*sn*-glycero-3-phosphatidylcholine (DMPC)/3-[(cholamidopropyl)-dimethylammonio]-1-propanesulfonate) (CHAPS) micelles (Booth et al., 1997), since time-resolved CD experiments indicate the formation of secondary structure elements in the submillisecond time domain. It most probably reflects the formation of secondary structure elements at the surface of the membrane/micelle. The second relaxation phase (corresponding to the fast phase, k_2, visible in both mutants) then corresponds to the insertion of helices I + II and III + IV as hairpins into the micelle.

Some rearrangement of the loop between helices II and III may be responsible for the slowest process visible in the wild-type and mutant W77F. This process probably reflects the dimerization of OEP16 monomers to a functional channel protein as well. It can only be followed by fluorescence when Trp-100 is present. The graph of the amplitudes of the fast and the slow processes as functions of the detergent concentration (Fig. 4 *c*) displays saturation of the amplitude of the fast signal, k_2, at high concentrations, whereas the slowest process has its maximum close to the CMC of $C_{12}E_8$ and declines with higher detergent concentrations. Either a loop rearrangement becomes obsolete in higher detergent concentrations because the loop instantly folds in the correct way or, if the dimerization of OEP16 can indeed be monitored by Trp-100, this dimerization might be hindered by higher detergent concentrations. On the other hand, dimerization should be favored at higher protein concentrations, but the time constant of the second process does not significantly change with rising concentrations of OEP16. Thus it seems more probable that low detergent concentrations can lead to the formation of a short-lived folding intermediate in this small α-helical membrane protein. In that case, the rearrangement is the rate limiting step of the folding reaction. Correct folding during helix insertion becomes more favorable with higher detergent concentrations, resulting in smaller amplitudes of the slowest process.

This work was supported by the Deutsche Forschungsgemeinschaft project FR 320/3-2.

REFERENCES

Abornev, S. M., and E. A. Burstein. 1992. Resolution of protein tryptophan fluorescence spectra into elementary components. *Mol. Biol.* 26:890–897.

Block, M. A., A.-J. Dorne, J. Joyard, and R. Douce. 1983. Preparation and characterization of membrane fractions enriched in outer and inner

envelope membranes from spinach chloroplasts. *J. Biol. Chem.* 258: 13281–13286.

Bölter, B., J. Soll, K. Hill, R. Hemmler, and R. Wagner. 1999. A rectifying ATP-regulated solute channel in the chloroplastic outer envelope from pea. *EMBO J.* 18:5505–5516.

Booth, P. J., and A. R. Curran. 1999. Membrane protein folding. *Curr. Opin. Struct. Biol.* 9:115–121.

Booth, P. J., M. L. Riley, S. L. Flitsch, R. H. Templer, A. Farooq, A. R. Curran, N. Chadborn, and P. Wright. 1997. Evidence that bilayer bending rigidity affects membrane protein folding. *Biochemistry.* 36: 197–203.

Bradford, M. M. 1976. A rapid and sensitive method for the quantitation of microgram quantities of protein utilizing the principle of protein-dye binding. *Anal. Biochem.* 72:248–254.

Buchanan, S. K. 1999. β-Barrel proteins from bacterial outer membranes: structure, function and refolding. *Curr. Opin. Struct. Biol.* 9:455–461.

Bukolova-Orlova, T. G., E. A. Burstein, and L. Y. Yukelson. 1974. Fluorescence of neurotoxins from Middle-Asian cobra venom. *Biochim. Biophys. Acta.* 342:275–280.

Burstein, E. A. 1983. Intrinsic protein luminescence as a tool of studying the fast structural dynamics. *Mol. Biol.* 17:455–467.

Burstein, E. A., S. M. Abornev, and Y. K. Reshetnyak. 2001. Decomposition of protein tryptophan fluorescence spectra into log-normal components: algorithms of the decomposition. *Biophys. J.* 81: 1699–1709.

Burstein, E. A., and V. I. Emelyanenko. 1996. Log-normal description of fluorescence spectra of organic fluorophores. *Photochem. Photobiol.* 64:316–320.

Bushueva, T. L., E. P. Busel, V. N. Bushuev, and E. A. Burstein. 1974. The interaction of protein functional groups with indole chromophore. I. Imidazole group. *Stud. Biophys.* 44:129–132.

Callebaut, I., G. Labesse, P. Durand, A. Poupon, L. Canard, J. Chomilier, B. Henrissat, and J. P. Mornon. 1997. Deciphering protein sequence information through hydrophobic cluster analysis (HCA): current status and perspectives. *Cell. Mol. Life Sci.* 53:621–645.

Cline, K., and R. Henry. 1996. Import and routing of nucleus-encoded chloroplast proteins. *Annu. Rev. Cell Dev. Biol.* 12:1–26.

Danino, D., Y. Talmon, and R. Zana. 1997. Aggregation and microstructure in aqueous solutions of the nonionic surfactant C12E8. *J. Colloid Interface Sci.* 186:170–179.

Flügge, U. I. 1998. Metabolite transporters in plastids. *Curr. Opin. Plant Biol.* 1:201–206.

Flügge, U. I. 2000. Transport in and out of plastids: does the outer envelope membrane control the flow? *Trends Plant Sci.* 5:135–137.

Froehlich, J. E., C. Benning, and P. Dörmann. 2001. The digalactosyldiacylglycerol (DGDG) synthase DGD1 is inserted into the outer envelope membrane of chloroplasts in a manner independent of the general import pathway and does not depend on direct interaction with monogalactosyldiacylglycerol synthase for DGDG biosynthesis. *J. Biol. Chem.* 276: 31806–31812.

Heins, L., I. Collinson, and J. Soll. 1998. The protein translocation apparatus of chloroplast envelopes. *Trends Plant Sci.* 3:56–61.

Joyard, J., M. A. Block, and R. Douce. 1991. Molecular aspects of plastid envelope biochemistry. *Eur. J. Biochem.* 199:489–509.

Kleinschmidt, J. H., and L. K. Tamm. 1996. Folding intermediates of a β-barrel membrane protein. Kinetic evidence for a multi-step membrane insertion mechanism. *Biochemistry.* 35:12993–13000.

Kuni, F. M., A. P. Grinin, A. K. Shchekin, and A. I. Rusanov. 2001a. Thermodynamic and kinetic foundations of the micellization theory: 4. Kinetics of establishment of equilibrium in a micellar solution. *Colloid Journal.* 63:197–204.

Kuni, F. M., A. I. Rusanov, A. P. Grinin, and A. K. Shchekin. 2001b. Thermodynamic and kinetic foundations of the micellization theory: 5. Hierarchy of kinetic times. *Colloid Journal.* 63:723–730.

Linke, D. 2002. Structure and function of a pore protein of the chloroplast outer envelope. Thesis. Technische Universität Berlin, Berlin, Germany.

Linke, D., J. Frank, J. F. Holzwarth, J. Soll, C. Boettcher, and P. Fromme. 2000. In vitro reconstitution and biophysical characterization of OEP16, an outer envelope pore protein of pea chloroplasts. *Biochemistry.* 39: 11050–11056.

Pohlmeyer, K., J. Soll, R. Grimm, K. Hill, and R. Wagner. 1998. A high-conductance solute channel in the chloroplastic outer envelope from pea. *Plant Cell.* 10:1207–1216.

Pohlmeyer, K., J. Soll, T. Steinkamp, S. Hinnah, and R. Wagner. 1997. Isolation and characterization of an amino acid-selective channel protein present in the chloroplastic outer envelope membrane. *Proc. Natl. Acad. Sci. USA.* 94:9504–9509.

Rassow, J., P. J. T. Dekker, S. van Wilpe, M. Meijer, and J. Soll. 1999. The preprotein translocase of the mitochondrial inner membrane: function and evolution. *J. Mol. Biol.* 286:105–120.

Reshetnyak, Y. K., and E. A. Burstein. 2001. Decomposition of protein tryptophan fluorescence spectra into log-normal components. II. The statistical proof of discreteness of tryptophan classes in proteins. *Biophys. J.* 81:1710–1734.

Reshetnyak, Y. A., Y. Koshevnik, and E. A. Burstein. 2001. Decomposition of protein tryptophan fluorescence spectra into log-normal components. III. Correlation between fluorescence and microenvironment parameters of individual tryptophan residues. *Biophys. J.* 81:1735–1758.

Schulz, G. E. 2000. β-Barrel membrane proteins. *Curr. Opin. Struct. Biol.* 10:443–447.

Soll, J., B. Bölter, R. Wagner, and S. C. Hinnah. 2000. Response: the chloroplast outer envelope: a molecular sieve? *Trends Plant Sci.* 5:137–138.

Steinkamp, T., K. Hill, S. C. Hinnah, R. Wagner, T. Röhl, K. Pohlmeyer, and J. Soll. 2000. Identification of the pore-forming region of the outer chloroplast envelope protein OEP16. *J. Biol. Chem.* 275:11758–11764.

Timmins, P., E. Pebay-Peroula, and W. Welte. 1994. Detergent organization in solutions and in crystals of membrane proteins. *Biophys. Chem.* 53:27–36.